J Mater Sci (2011) 46:3653–3658
DOI 10.1007/s10853-011-5282-5

Yield strength enhancement of martensitic steel through titanium addition

L. Xu · J. Shi · W. Q. Cao · M. Q. Wang · W. J. Hui · H. Dong

Received: 15 December 2010 / Accepted: 12 January 2011 / Published online: 25 January 2011

Abstract Yield strength enhancement for martensitic steel fabricated by vacuum induction melting is investigated. It is found that the addition of Ti can improve the yield strength property of the martensitic steel, which can be attributed to increase in precipitation hardening from formation of TiC precipitates in the martensitic matrix. Moreover, the yield strength can be further enhanced by tempering and reheat quenching process, which can be ascribed to the formation of a superfine sized ($\sim$8 μm) grains and large amount of freshly nano-sized (1–10 nm) precipitates in the final martensitic structure for martensitic steel containing Ti. The experimental and theoretical results on the contribution of TiC precipitates to hardening of the martensitic steel are in excellent agreement, showing that the precipitation hardening of 188 MPa caused by TiC precipitates is the main reason why the yield strength for martensitic steel is enhanced via titanium addition.

Introduction

Martensitic steels are very important metallic materials. Their outstanding properties are high strength [1], excellent ductility [2], and good weldability [3], which are used in a variety of applications, including pipelines [4], gas turbines [5], compressor wheels, blades [6], bolts, and sheet structures [7]. The strength of conventional martensitic steel was mainly related to its carbon content [8, 9] and alloy content [10, 11]. However, it is well known that precipitation hardening [12] and grain refinement hardening [13] is also a promising approach to increase the strength of steels but few studies is carried out in the martensitic steels at present time. Therefore, further investigation is required to promote our understanding of these phenomena.

As a transition metal, titanium has numerous attractive properties, such as low density, good strength [14], which is also a strong carbide-forming element. It was expostulated that the titanium carbide precipitates can not only improve the strength by precipitation hardening but also refine the grain size by pinning of precipitation. Based on this idea, the martensitic steel containing Ti to form precipitates was designed and fabricated by vacuum induction melting. The precipitation hardening and grain refinement, caused by TiC precipitates and their effect on the yield strength of martensitic steel during heat treatment, are reported.

Experimental

Table 1 shows the chemical compositions of the designed steel used in this study. The steel was fabricated by vacuum induction melting. The ingots were homogenized at 1250 °C with 2 h, forged in between 1200 and 850 °C into a plate of 30 × 200 × 100 mm. The hot-rolling simulation was done using a pilot mill with a prepared slab of 30 mm in thickness. The basic thermomechanical pattern was shown in Fig. 1. The slab was soaked at 1250 °C for 2 h in a muffle furnace and then hot rolled into strips of 7 mm in thickness through four passes. The plates were finally rolled at about 850 °C and water quenched to room temperature after final deformation. Then, the as-quenched plate was tempered at 550 °C with 3 h to investigate the effect of

L. Xu (✉) · J. Shi · W. Q. Cao · M. Q. Wang · W. J. Hui · H. Dong
National Engineering Research Center of Advanced Steel Technology (NERCAST), Central Iron and Steel Research Institute (CISRI), Beijing 100081, People's Republic of China
e-mail: never_stop_exploring@live.cn

Table 1 Chemical compositions of steel used (mass%)

C	Mn	Ti	B	P	S	[*N*]
0.2	1.5	0.16	0.003	0.005	0.004	0.003

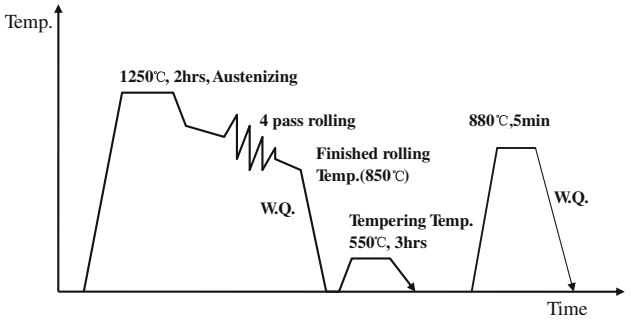

Fig. 1 The basic thermomechanical pattern for samples

the tempering on the precipitation. After the tempering process, the plate was soaked at 880 °C for 5 min in a muffle furnace and water quenched to room temperature to obtain the martensitic matrix.

The microstructure was characterized by scanning electron microscopy (SEM), and transmission electron microscopy (TEM). A HITACHI S-4300 type scanning electron microscope and a HITACHI H-800 type transmission electron microscope were used. To reveal the prior austenite grains, the specimens were etched with a supersaturated picric acid aqueous solution after mechanical polishing. The prior austenite grain sizes in the experimental steel were determined by linear intercept measurements on optical micrographs. Thin-foil specimens for TEM observations were cut from the specimens and prepared by twin-jet electrolytic polishing using a solution of 10% perchloric acid and 90% ethanol at 243 K. The average diameter and size distribution of precipitates were analyzed and calculated by phase analysis method. Meanwhile, the phase structures of precipitates were identified by X-ray diffraction. Tensile test were performed on the dog-bone shape specimens with gauge length of 25 mm and diameter of 5 mm at a strain rate of 10^{-3}/s in an Instron machine at room temperature. For comparison, the mechanical properties of as-quenched Ti-killed martensitic steel with the same chemical compositions were also measured.

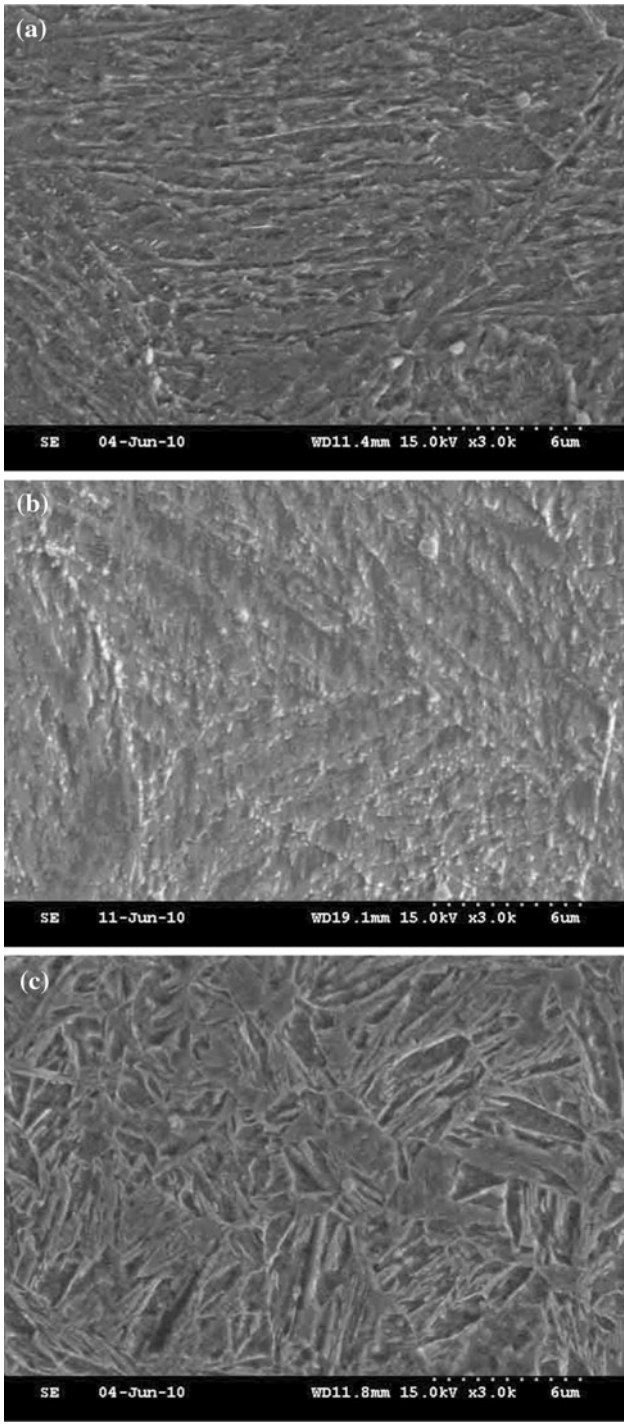

Fig. 2 SEM micrographs for **a** sample A, **b** sample B, and **c** sample C

Results and discussion

Figure 2 shows the SEM images for as-quenched sample A, tempered sample B, and reheat quenching sample C, respectively. Sample A exhibits the typical martensitic structure, while after tempering little carbides are visible in sample B, but the boundary of lath-martensite becomes unclear. As for sample C, the microstructure is also martensitic structure, but it is obvious refinement comparing to the sample A. This implies that the reheat quenching process can refine the martensitic texture, and the tempered

martensite with carbides can be obtained by tempering for 3 h at 550 °C.

Figure 3 exhibits the TEM images for samples A–C. The relative bulky precipitates can be observed in sample A (Fig. 3a), which is attributed to precipitate in austenite during the hot rolling process. However, as the tempering process introduced the density of precipitates in tempering sample B (Fig. 3b) becomes higher. As for sample C (Fig. 3c), the size and density of precipitates change remarkably when compared with samples A and B. The sample C has the maximum density of precipitates during these three samples. In order to investigation the quality and quantity of the precipitates for these samples, the XRD patterns and the phase analysis results of precipitates are shown in Fig. 4 and Table 2. From Fig. 4, the peaks at $2\theta = 35°$, 40.8°, 49°, 71° from TiC [15–17] (111), (200), (220), (311) can be found in the XRD patterns (Fig. 4) for samples A–C, which imply that the main precipitates of these samples are the TiC phase. It is interesting that other peaks also appear in addition to the peak from TiC in Fig. 4b. The peaks at $2\theta = 48.5°$, 53°, 58° can be ascribed to Fe_3C (220), (202) and (231), respectively. Table 2 shows that the precipitation content of Ti in samples A, B, and C is 0.092, 0.139, and 0.16%, respectively. It seems that different heat treatment processes can make the Ti precipitate in different contents.

Figure 5 shows the size distribution of TiC precipitates for samples A–C. From this figure, it can be seen that the mass fraction of TiC precipitates in diameter from 30 to

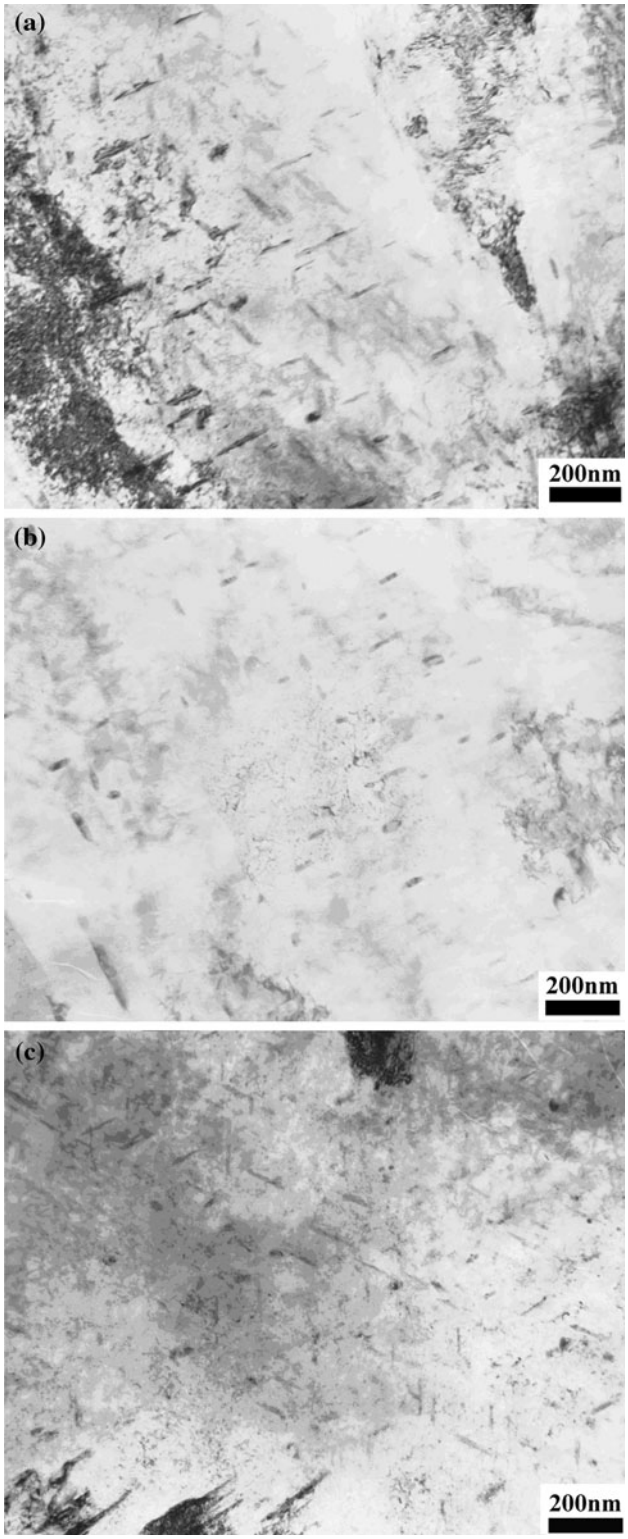

Fig. 3 TEM images for **a** sample A, **b** sample B, and **c** sample C

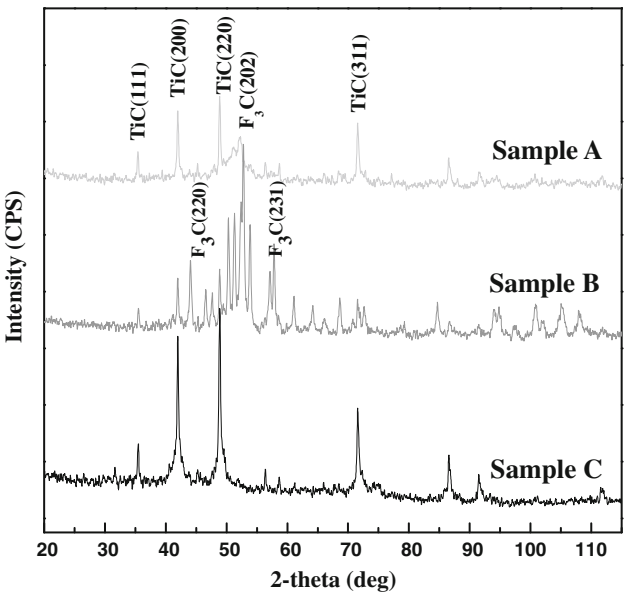

Fig. 4 The XRD patterns for samples A–C

Table 2 The phase analysis results for samples A–C (mass%)

Sample	A	B	C
Precipitation content of Ti	0.092	0.139	0.16
Precipitation content of C	0.023	0.035	0.04

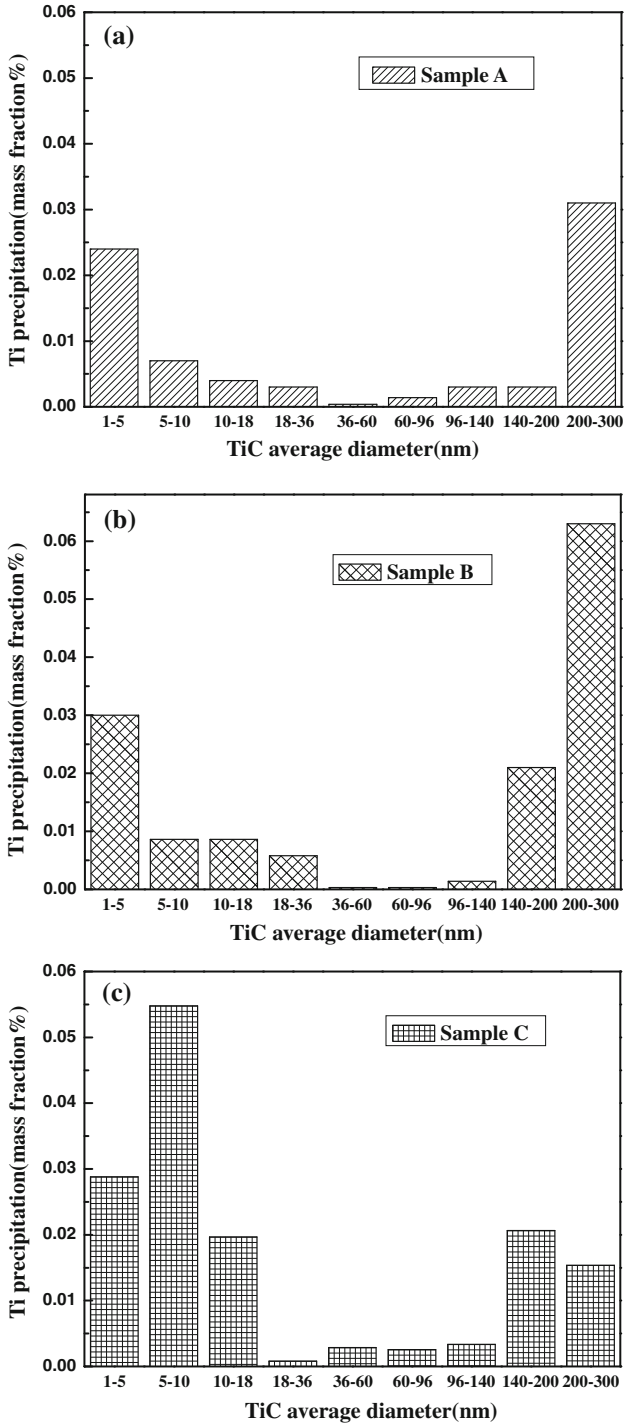

Fig. 5 The size distribution and precipitation content of TiC in **a** sample A, **b** sample B, and **c** sample C

100 nm does not change too much during these three samples. However, the mass fraction of TiC precipitates in diameter from 1 to 10 nm changes significantly under different heat treatments. The sample A has the lowest mass fraction of fine TiC precipitates in diameter from 1 to 10 nm. In contrast, sample C has the highest mass fraction of TiC precipitates in diameter from 1 to 10 nm during those three samples. It is interesting that the mass fraction of relative bulky size TiC precipitates in diameter with 140–300 nm decreases in sample C after reheat quenching process compared with other two samples. From the previously given results, it is not difficult to understand that the size distribution of TiC precipitates can be significantly influenced by the heat treatment. A large number of freshly nano-sized (1–10 nm) TiC precipitates are formed only in the reheat quenching sample C, rather than as-quenched sample A.

Table 3 shows the mechanical properties from as-quenched sample A, tempered sample B, reheat quenching sample C, Ti-killed sample, respectively, in which the yield strength from the measured samples is 1220, 1100, 1280, 1160 MPa. This means that the as-quenched sample A has a better yield strength than that of Ti-killed sample, and the sample C has the best yield strength among four samples. It seems that a proper Ti addition is favorable to improve the yield strength for martensitic steel, and the yield strength of Ti containing martensitic steel can be further enhanced by tempering and reheat quenching treatment. Meanwhile, the total elongation and reduction of area also have been improved slightly after Ti addition in the present martensitic steel.

Comparing as-quenched sample A with as-quenched Ti-killed sample, the yield strength has been enhanced by Ti addition. As we know, the microstructure of the steel after quenching treatment was martensite, and, thus, martensitic hardenability is not considered to be a factor in these strength differences between the two samples. The average grain size is also an important factor to influence the yield strength of martensitic steel. Figure 6 shows that there is no appreciable difference in the average grain size between sample A (Fig. 6a) and Ti-killed sample (Fig. 6c). Therefore, the yield strength enhancement effect induced by average grain size can be negligible in the present case. Table 2 shows that there is 0.092% Ti precipitation in sample A, which may cause precipitation hardening in the martensitic steel. It is well known that the yield strength of steels contain a contribution from the precipitation hardening, which is also described quantitatively by the Ashby–Orowan equation. According to Ashby–Orowan relationship [18]

Table 3 The mechanical properties of samples

Sample	A	B	C	Ti-killed
Yield strength (MPa)	1220	1100	1280	1160
Total elongation (%)	12	14	13	11
Reduction of area (%)	55	60	57	56

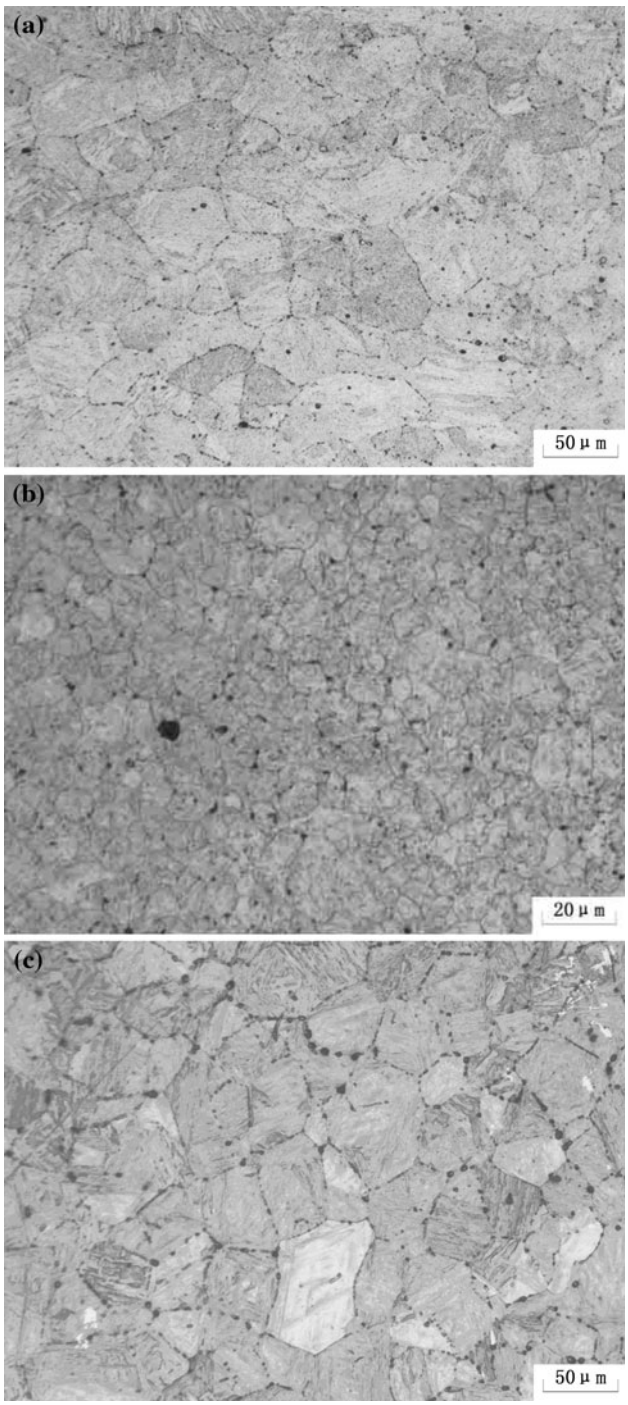

Fig. 6 The austenitic grain size images for **a** sample A, **b** sample C, and **c** Ti-killed sample

$$\sigma_p = (0.538Gbf^{1/2}/X)\ln(X/2b) \quad (1)$$

where σ_p is the increase in yield strength (MPa), G is the shear modulus (MPa), b is the Burgers vector (mm), f is the volume fraction of particles, and X is the real (spatial) diameter of the precipitates (mm). According to Eq. 1, substituting the value of the mass fraction and size distribution of TiC precipitates in Fig. 5a, the contribution from the precipitation hardening of sample A can be evaluated as 134 MPa. However, this precipitation hardening is counteracted by an unexpected softening mechanism, which is attributed to the formation of TiC precipitates making the content of carbon in martensitic matrix decrease. Phase analysis results show that the precipitation content of carbon is 0.023% (Table 2) in sample A, which can bring the strength decrease with 70 MPa in martensitic matrix [19]. Then, the difference between precipitation hardening from TiC and decrease solid solution from carbon is the actual yield strength enhancement, i.e., 60 MPa for sample A, which agrees well with the experimental results. Therefore, the yield strength enhancement of martensitic steel in the present case can be mainly attributed to precipitation hardening after Ti addition.

The yield strength of reheat quenching sample C, compared to as-quenched sample A, has been further improved. One possible reason may be attributed to the different average grain sizes. Figure 6 shows that there is significant difference in the average grain size between as-quenched A (Fig. 6a) and reheat quenching sample C (Fig. 6b). The average grain size of sample C is about 8 μm (Fig. 6b), which is relatively smaller than that of sample A with 43 μm (Fig. 6a). It is well known that the grain refinement can enhance yield strength of the steel. The smaller the average grain size is the better is the yield strength. Therefore, one reason of the yield strength enhancement for sample C in the present case is grain refinement, which is mainly attributed to the TiC precipitates pinning austenitic grain boundaries during the reheat quenching process, favoring for reducing grain size. According to the conventional Hall–Petch equation [20]:

$$\sigma_y = Kd^{-1/2} + \sigma_0 \quad (2)$$

From Eq. 2, the value of contribution of grain refinement can be estimated as 80 MPa, which may imply that the grain refinement after reheat quenching is a reason for the yield strength enhancement for sample C. Concerning precipitates in this steel, most of the TiC precipitates present in the as-quenched steel should dissolve during the 1250 °C treatment prior to hot rolling. As a result, Ti is available for precipitation during subsequent process. Because the plates were finish rolled below about 850 °C, it is hypothesized that TiC precipitates formed on the deformation substructure of the austenite, thereby inhibiting austenite recrystallization. For the sample A, the steel plate was immediately quenched after hot rolling. As a result of quenching, it is expected that the titanium-containing substructure precipitates remain relatively fine. Additionally, a significant portion of titanium remains in solid solution. Subsequent tempering at 550 °C would result in freshly formed TiC precipitates (Fig. 5b), finer

Table 4 The dislocation density of samples A–C after deformation

Sample	A	B	C
Dislocation density (deformed)	3.6×10^{11}	1.7×10^{10}	5.6×10^{11}
Dislocation density (undeformed)	8.8×10^{10}	7.7×10^{9}	1.8×10^{11}

than the substructure precipitates discussed above, as well as coarsening of any pre-existing precipitates (Fig. 5b). During reheat quenching process, the relative bulky precipitates dissolved again and freshly formed fine TiC precipitates appear on the order of 1–10 nm in diameter (Fig. 5c), which may play an important role in the yield strength enhancement. According to Eq. 1, the contribution from the precipitation hardening of sample C can be evaluated as 188 MPa, which is higher ~50 MPa than that of sample A. Meanwhile, the 0.04% carbon precipitation (Table 2) causes the strength decrease with 150 MPa in martensitic matrix [19]. Then, the difference between precipitation hardening and grain refinement from TiC precipitates and decrease solid solution from carbon is the actual yield strength enhancement, i.e., 60 MPa for sample C, which agrees well with the experimental results. Therefore, the yield strength enhancement of reheat quenching sample C compared with as-quenched sample A in the present case can be mainly attributed to precipitation hardening and grain refinement from TiC precipitates after reheat quenching process. It is well known that the precipitation hardening is attributed to the precipitates act as obstacles to dislocation movement, raising dislocation density during the deformation. The dislocation density of deformed sample C shown in Table 4 is higher than that of other deformed samples, where it is relatively same before deformation. Our results suggest that the precipitation hardening in sample C can be ascribed to the fine TiC precipitates hindering the dislocation movement and making dislocation multiplication during deformation.

Conclusions

The effect of Ti addition on the yield strength for martensitic steel fabricated by vacuum induction melting has been investigated. It is found that the yield strength properties of martensitic steel can be improved by Ti addition, which is associated with precipitation hardening from formation of TiC precipitates in the martensitic matrix. Furthermore, it is found that the tempering and reheat quenching treatment can promote a formation of freshly nano-sized TiC in diameter from 1 to 10 nm and refine the average grain size to a superfine sized (~8 μm) grains and lead to a further increase in the yield strength for martensitic steel containing Ti, and the theoretical calculations are used to explain the yield strength enhancement. The results show that the formation of nano-sized precipitates after reheat quenching process act as obstacles to dislocation movement, which can result in precipitation hardening of 188 MPa overshadowing the grain refinement of 80 MPa. This investigation sheds a deep light on the precipitation hardening and grain refinement for martensitic steel containing Ti under different heat treatments.

Acknowledgements This research is supported by National Basic Research Program of China (973 program) No. 2010CB630803 and National High-tech R&D Programs (863 programs) No. 2511 and No. 2009AA033401.

References

1. Abd-Allah NM, El-Fadaly MS, Megahed MM, Eleiche AM, Mater J (2001) Eng Perform 10:576
2. Ezugwu EO, Olajire KA (2002) Tribol Lett 12:183
3. Yilmaz R, Türkyilmazoglu A (2007) Adv Mater Res 23:319
4. Bhavsar RB, Montani E (1998) Corrosion 98:22
5. Oliver DA, Harris GT (1952) Iron Steel Inst 43:46
6. Davies WT, Hall B (1967) The Iron and Steel Inst 97:561
7. Angeliu T, Hall EL, Larsen M, Linsebigler A, Mukira C (1999) Inst Mater 708:234
8. Parameswaran P, Vijayalakshmi M, Shankar P, Raghunathan VS (1992) J Mater Sci 27:5426. doi:10.1007/BF00367811
9. Martin R, Mari D, Schaller R (2009) Mater Sci Eng A 521–522: 117
10. Song YY, Ping DH, Yin FX, Li XY, Li YY (2010) Mater Sci Eng A 527:614
11. Bhambri SK (1986) J Mater Sci 21:1741. doi:10.1007/BF01114734
12. Ikeda S, Sakai T, Fine ME (1977) J Mater Sci 12:675. doi:10.1007/BF00548157
13. Barani AA, Li F, Romano P, Ponge D, Raabe D (2007) Mater Sci Eng A 463:138
14. Yaggee FL, Gilbert ER, Styles JW (1969) J Less Common Met 19:39
15. Baviera P, Harel S, Garem H, Grosbras M (2001) Scripta Mater 44:2721
16. Mani A, Aubert P, Mercier F, Khodja H, Berthier C, Houdy P (2005) Surf Coat Technol 194:190
17. Li SB, Xiang WH, Zhai HX, Zhou Y (2008) Powder Technol 185:49
18. Cao JC, Yong QL, Liu QY, Sun XJ (2007) J Mater Sci 42:10080. doi:10.1007/s10853-007-2000-4
19. Sagaradze VS (1970) Met Sci Heat Treat 12:198
20. Friedman LH, Chrzan DC (1998) Phys Rev Lett 83:2715